Talanta 184 (2018) 513–519

Contents lists available at ScienceDirect

Talanta

journal homepage: www.elsevier.com/locate/talanta

Detection and differentiation of Cys, Hcy and GSH mixtures by ^{19}F NMR probe

Shengjun Yang[a], Qingbin Zeng[a], Qianni Guo[a], Shizhen Chen[a], Hongbin Liu[a], Maili Liu[a], Michael T. McMahon[b], Xin Zhou[a,*]

[a] Key Laboratory of Magnetic Resonance in Biological Systems, State Key Laboratory of Magnetic Resonance and Atomic and Molecular Physics, National Center for Magnetic Resonance in Wuhan, Wuhan Institute of Physics and Mathematics, Chinese Academy of Sciences, Wuhan 430071, China
[b] Department of Radiology and Radiological Sciences, Johns Hopkins School of Medicine and F.M. Kirby Research Center for Functional Brain Imaging, Kennedy Krieger Institute, Baltimore, MD 21205, USA

ARTICLE INFO

Keywords:
^{19}F nuclear magnetic resonance
Biothiols
Probes
Thiol-addition/intramolecular cyclization

ABSTRACT

Simultaneous detection and differentiation of biomolecules is of significance in biological research. Biothiols such as cysteine (Cys), homocysteine (Hcy), and glutathione (GSH) play an important role in regulating the vital functions of living organisms. However, existing methods for simultaneous detection and differentiation of Cys, Hcy, and GSH are still challenging because of their similarity in structure and chemical properties. Herein we report a probe that simultaneously detects and discriminates between mixtures of Cys, Hcy and GSH using ^{19}F nuclear magnetic resonance (NMR). This ^{19}F NMR probe responds rapidly to biothiols through the Michael addition reaction and subsequent intramolecular cyclization reaction allowing differentiation between Cys, Hcy and GSH through ^{19}F NMR chemical shift. We demonstrate that this ^{19}F NMR probe is a powerful method for analysis of complex mixtures.

1. Introduction

Simultaneous detection and differentiation of biologically important molecules are vital in clinical diagnosis. Biothiols, such as cysteine (Cys), homocysteine (Hcy) and glutathione (GSH), are widely existing intracellular biomolecules, which have been documented as playing significant roles in many physiological and pathological processes [1]. Cys and Hcy have been regarded as risk factors for several health problems. For example, elevated levels of Cys could lead to neurotoxicity, and the deficiency in Cys associate with the syndromes of skin lesions, liver damage, lethargy, hair depigmentation, and weakness [2]. GSH, the most abundant intracellular biothiol, serves as an essential endogenous antioxidant for maintaining redox homeostasis, intracellular signal transduction and gene regulation through the equilibrium of free thiols and oxidized disulfides [3]. The aberrant level of GSH have also been documented to correlate with several diseases, such as liver damage, leucocyte loss, psoriasis, cancer, and HIV infection [4].

Over the past few decades, the usage of high performance liquid chromatography, [5,6] capillary electrophoresis, [7,8] voltammetry, [9,10] flow injection, [11,12] mass spectrometry identification, [13–15] ^{129}Xe Nuclear magnetic resonance (NMR) [16,17] and fluorescence [18–20] have been applied for the development of biothiol sensing. Among them, fluorescence probes based on thiol-selective reactions, including the Michael addition reaction, cyclization reaction, cleavage reaction of sulfonamide, sulfonate esters, selenium–nitrogen bonds, and disulfide bonds by thiol, nucleophilic substitution reaction, and others have become a popular approach for biothiol detection in living cells [21–33]. Some impressive fluorescence probes have been successfully developed to discriminate biothiols using different emission channels. However, fluorescent probes that can fully and simultaneously discriminate these three sulfhydryl-containing amino acids are quite rare owing to the existence of similarities in structures and reaction activities. In this context, the development of a probe for biothiols detection, especially simultaneous discrimination one thiol species from another in mixtures is of highly practical value but more challenging in biological studies.

Nuclear magnetic resonance spectroscopy is a versatile tool widely used for studying the information of precise structures and dynamic reaction events. Sensors based on the proton NMR have been developed that employ modulation of relaxation rates or chemical shifts upon binding [34–43]. Although promising, such water proton based sensors often subject to the lack of chemical selectivity or narrow chemical shift range. On the other hand, ^{19}F NMR spectroscopy has emerged as a promising approach, as not only it holds the advantages of high

* Corresponding author.
E-mail address: xinzhou@wipm.ac.cn (X. Zhou).

https://doi.org/10.1016/j.talanta.2018.03.039
Received 7 October 2017; Received in revised form 2 March 2018; Accepted 14 March 2018
Available online 15 March 2018
0039-9140/

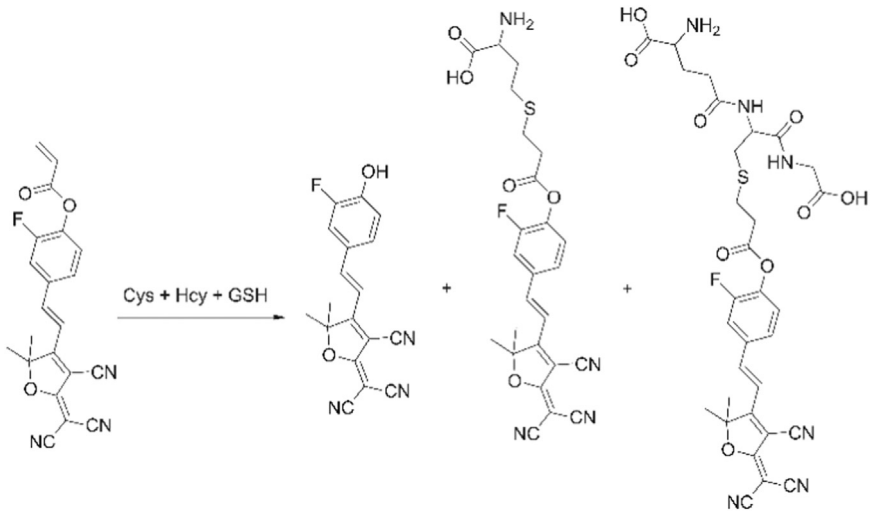

Scheme 1. Illustration of ^{19}F NMR probe 1 simultaneously differentiation of Cys, Hcy and GSH.

sensitivity in NMR spectroscopy (83% relative to ^{1}H), 100% natural abundance, no background interference in human cells and tissues, but also the broad chemical shift range is typically an order of magnitude greater than that of proton NMR spectroscopy [44,45]. Such advantages have been successfully used for in vitro and in vivo detection and imaging of biological species of interest [46–58]. Recently, ^{19}F NMR has been applied in the detection and discrimination of complex mixtures. For example, Timothy Swager and coworkers designed a Tungsten Calix [4] arene Imido to differentiate the complex mixtures of neutral organic compounds using ^{19}F NMR in 2013 [59]. They further reported two palladium complexes for simultaneous sensing of multiple amines, neutral and anionic species without separation [60,61]. Therefore, ^{19}F NMR probes now constitute a promising strategy for differentiation of complex mixtures.

Herein, we report a reaction-based ^{19}F NMR probe for simultaneous detection and differentiation between mixtures of Cys, Hcy, and GSH. The working hypothesis here is subtle differences in Cys, Hcy and GSH could be differentiated by chemical shift upon reaction with ^{19}F NMR probe, producing observable ^{19}F signal changes (Scheme 1). To achieve this concept, we chose the acrylate group as a reaction site that is highly specific for response to biothiols [22–26]. More importantly, the acrylate group has been reported to be able to discriminate Cys from Hcy and GSH by different reaction rates in the conjugate addition and subsequently intramolecular cyclization reaction process, leading to preclude the interference of other species. In this manner, a fluorine atom functionalized at the *ortho*-position of acrylate group was introduced as the NMR signal moiety. Furthermore, 2-(3-cyano-4,5,5-trimethylfuran-2(5H)-ylidene)-malononitrile was also introduced as an optical signal output group.

2. Experimental section

2.1. Materials and instruments

Starting materials were purchased from commercial suppliers and used as received. NMR spectra were acquired on a Bruker AMX-500 NMR spectrometer at room temperature. The coupling constants (*J* values) are reported in hertz. Chemical shifts (δ) are given in parts per million (ppm) relative to internal TMS (0 ppm for ^{1}H) or DMSO-d_6 (39.5 ppm for ^{13}C). High-resolution mass spectrometry (HR MS-ESI) spectra were obtained on an Agilent technologies 6530 Accurate-Mass QTOF spectrometer coupled to an Agilent HPLC 1200 series. Uv–vis absorption spectra were recorded on an Evolution 220 spectrophotometer. Fluorescence spectra were obtained by an Edinburgh Instruments FS5 fluorescence spectrometer. pHs were measured by a Mettler Toledo SevenEasy pH meter. All solutions and buffers were prepared with distilled water that passed through a Millipore-Q ultrapurification system.

2.2. Synthesis and characterization of compound 2

To the solution of compound 3 [62,63] (288 mg, 1.45 mmol) in 10 mL of anhydrous ethanol in round flask, 3-fluoro-4-hydroxybenzaldehyde (210 mg, 1.50 mmol) and two drops of piperidine were added. After refluxed with stirring for 5 h, the reaction mixture was cooled down to room temperature and the precipitate was filtered off, washed with ethanol to give the desired compound 2 (67% yield). ^{1}H NMR (500 MHz, DMSO-d_6): δ 1.78 (6 H, s), 7.06 (1H, t, J = 8.5 Hz), 7.09 (1H, d, J = 16.5 Hz), 7.59 (1H, dd, J = 8.5 Hz, 2.0 Hz), 7.86 (1H, d, J = 16.5 Hz), 7.91 (1H, dd, J = 12.5 Hz, 2.0 Hz), 11.05 (1H, s). ^{13}C NMR (125 M Hz, DMSO-d_6): δ 177.7, 175.9, 152.7, 150.7, 150.1, 150.0, 147.5, 147.4, 128.6, 126.8, 126.8, 118.6, 118.6, 117.2, 117.1, 113.8, 113.3, 112.5, 111.5, 99.7, 98.1, 54.2, 25.6. HRMS (ESI): *m/z* calcd. For $C_{18}H_{12}FN_3O_2Na^+$ $[M+Na]^+$ 344.0806, found 344.0810.

2.3. Synthesis and characterization of compound 1

To the solution of compound 2 (96 mg, 0.30 mmol) and triethylamine (121 μL, 0.87 mmol) in CH_2Cl_2, acryloyl chloride (70 μL, 0.86 mmol) was added with stirring at room temperature. After the reaction completed, the mixture was concentrated under reduced pressure. The crude product was redissolved in ethanol and crystallized to give the desired probe 1 (77% yield). ^{1}H NMR (500 M Hz, DMSO-d_6): δ 1.80 (6H, s), 6.27 (1H, dd, J = 10.5 Hz, 1.0 Hz), 6.48 (1H, dd, J = 17.5 Hz, 10.5 Hz), 6.63 (1H, dd, J = 17.5 Hz, 1.0 Hz), 7.30 (1H, d, J = 16.5 Hz), 7.52 (1H, t, J = 8.2 Hz), 7. 82 (1H, dd, J = 8.5 Hz, 1.5 Hz), 7.88 (1H, d, J = 16.5 Hz), 8.12 (1H, dd, J = 11.5 Hz, 2.0 Hz). ^{13}C NMR (125 MHz, DMSO-d_6): δ 177.5, 175.0, 163.4, 155.2, 153.2, 145.2, 145.2, 140.4, 140.3, 135.8, 134.7, 134.7, 127.4, 127.3, 126.8, 125.4, 117.4, 117.2, 117.0, 113.1, 112.2, 111.1, 101.0, 100.0, 55.4, 25.5. HRMS (ESI): *m/z* calcd. For $C_{21}H_{14}FN_3O_3Na^+$ $[M+Na]^+$ 398.0911, found 398.0920.

2.4. Absorption, fluorescence and ^{19}F NMR spectra studies

Probe 1 was dissolved into Acetonitrile (HPLC grade) to prepare the stock solution with a concentration of 1.0 mM. Stock solutions of analytes including Cys, Hcy, GSH, $Na_2S_2O_3$, Threonine, Serine, Leucine, Sodium erythorbate, K_2SO_8, Glutamine, Tyrosine, Lysine, Glycine, Methionine, Aspartic acid, Tryptophan, Pyroglutamic acid,

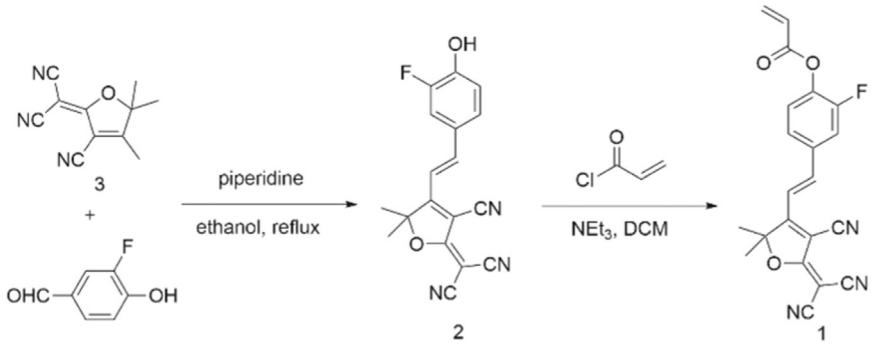

Scheme 2. Synthesis of the probe 1.

Phenylalanine, phenylglycine were prepared in a certain concentration using distilled water. After diluted to the desired concentration, probe 1 was added various other analytes. The resulting solution was well-mixed and prepared for the spectra measurement at 25 °C. For ^{19}F NMR spectra, unless stated otherwise, all the ^{19}F NMR spectra were processed with the line broadening of 10 Hz.

3. Result and discussion

3.1. Probe synthesis

The synthetic route for probe 1 is outlined in Scheme 2. As depicted, probe 1 was easily synthesized in two steps with good yield. Briefly, it can be obtained simply by the reaction of acryloyl chloride with compound 2 under basic conditions at room temperature. The structure of probe 1 was fully characterized by ^{1}H NMR, ^{13}C NMR, and HRMS as shown in the Supporting Information (SI). Compound 2 can be obtained by the condensation of 2-(3-cyano-4,5,5- trimethylfuran-2(5H)-ylidene)-malononitrile and 3-fluoro-4-hydroxybenzaldehyde according to the literature method [62,63]

3.2. Absorption and fluorescence detection of biothiols

With probe 1 in hand, the initial experiments explored the sensing potential for biothiols by optical method. Probe 1 (10 μM) shows a light-yellow color in 20 mM HEPES (HEPES = 2-[4-(2-hydroxyethyl)-1-piperazinyl]-ethanesulfonic acid, pH = 7.4) buffer solution with 30% acetonitrile and 5% D_2O as cosolvent. When 10 equiv. of Cys was added to probe 1, the color of this solution changed rapidly to colorless and afterwards progressively turned to purple, which can be easily distinguished by naked eye (Fig. S1).

Based on the above results, more details on the response of probe 1 for biothiols were investigated on Uv–vis and fluorescence spectrometers. Probe 1 (10 μM) exhibits a moderately strong maximum absorption peak centered at 398 nm. After addition of 10 equiv. of Cys, the absorption peak at 398 nm decreased rapidly together with the appearance of a new peak at 340 nm. Concomitantly, another strong band centered at 587 nm emerged and increased gradually until it reached a plateau in about 90 min (Fig. 1a). The fluorescence intensity of probe 1 was found to be weak (Fig. 1b). After addition of 10 equiv. of Cys, this intensity of probe 1 at 615 nm gradually increased with time until it reached emission saturation in about 90 min. Additionally, the scanning kinetics studies of fluorescence indicated that probe 1 is reasonably stable under the test conditions, and further verified that reaction of probe 1 with 10 equiv. Cys completed within 90 min (Fig. S2).

In the case of GSH and Hcy, although the absorption peak at 398 nm decreased rapidly and simultaneously a new peak around 340 nm appeared after addition, the absorption intensity at 587 nm did not display the same significant enhancement as that of Cys (Fig. S3). Similar results were also observed by using the fluorescence method. Upon addition, Hcy and GSH displayed enhancement in fluorescence intensity at 615 nm but not as significant as Cys (Fig. S4). On the other hand, scanning kinetics studies further revealed that the reaction of probe 1 with Cys is faster than Hcy and GSH. The according apparent rate constant of probe 1 with 10 equiv. Cys is 0.049 min^{-1}, which is over 10 times larger than that of Hcy (k = 0.0046 min^{-1}) and GSH (k = 0.0023 min^{-1}) (Fig. S5).

Furthermore, selectivity was investigated by Uv–vis absorption and fluorescence (Fig. S6). In both Uv–vis absorption and fluorescence spectra, Cys induced the most significant absorption and fluorescence intensity change. However, other test species including $Na_2S_2O_3$, Threonine, Serine, Leucine, Sodium erythorbate, K_2SO_8, Glutamine, Tyrosine, Lysine, Glycine, Methionine, Aspartic acid, Tryptophan, Pyroglutamic acid, Phenylalanine, Phenylglycine show almost no significant change.

All these results obtained by absorption and fluorescence methods suggest that probe 1 shows a specific response towards biothiols and can discriminate Cys from Hcy and GSH. It implies that probe 1 can be used as a potential colorimetric and fluorescence probe for Cys. However, it is inadequate to distinguish Hcy and GSH, and also the mixture of Cys, Hcy and GSH (Fig. S7). Therefore, new methods need to be developed for biothiols detection and Cys, Hcy and GSH simultaneous discrimination.

3.3. ^{19}F NMR study of probe 1 towards biothiols

The ^{19}F NMR spectrum of probe 1 (200 μM) shows one resonance at δ = − 127.6 ppm under the test conditions (Fig. 2). Notably, upon addition of 5 equiv. of Cys, the resonance at δ = − 127.6 ppm disappeared within 5 min and three new signals at δ = − 128.0 ppm, − 128.3 ppm and − 135.4 ppm were observed simultaneously. The results indicate that probe 1 was consumed completely within a few minutes and finally yielded a new product displaying the ^{19}F NMR signal at − 135.4 ppm via the intermediates of signals at − 128.0 ppm and − 128.3 ppm. The resonances at − 128.0 and − 128.3 ppm could be attributed to probe 1 undergoing the initial reaction of conjugate addition to acrylates of Cys to produce the intermediates, and the latter signal of − 135.4 ppm could be attributed to compound 2 which was produced by the subsequent intramolecular cyclization reaction. By recording the ^{19}F NMR spectra as a function of time, it was observed that the signals at δ = − 128.0 ppm and − 128.3 ppm decreased rapidly with concomitant growth of the signal at δ = − 135.4 ppm until it reached a saturation point. Obviously, ^{19}F chemical shift gives rise to the final up-field change of 7.8 ppm (from − 127.6 ppm to − 135.4 ppm) after the addition of Cys. A similar result was also observed upon addition of 3 equiv. of Cys (Fig. S8a). Furthermore, the signal at δ = − 135.4 ppm was still observed if lower concentrations of Cys (1 equivalent) were added, but the signal at δ = − 127.6 ppm decreased much slower compared with the addition of 5 or 3 equivalent Cys (Fig. S8b).

Interestingly, differences were observed upon addition of Hcy and GSH. After the addition of 5 equivalents Hcy and GSH, the chemical

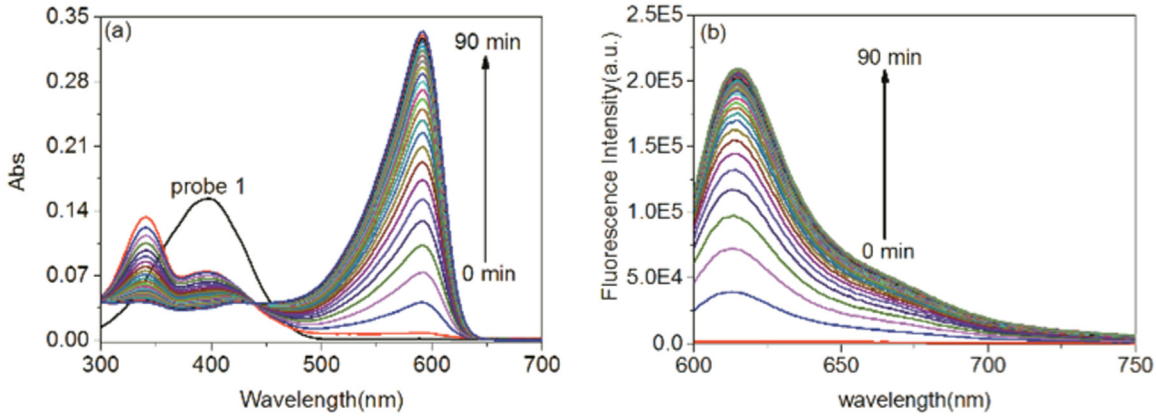

Fig. 1. Time-dependent (a) Uv–vis spectra and (b) fluorescence spectra changes of probe 1 (10 μM) upon addition of 10 equiv. of Cys. The spectra were collected from 0 to 90 min and conducted in HEPES buffer solution (pH 7.4, 20 mM) with 30% acetonitrile and 5% D_2O at 25 °C.

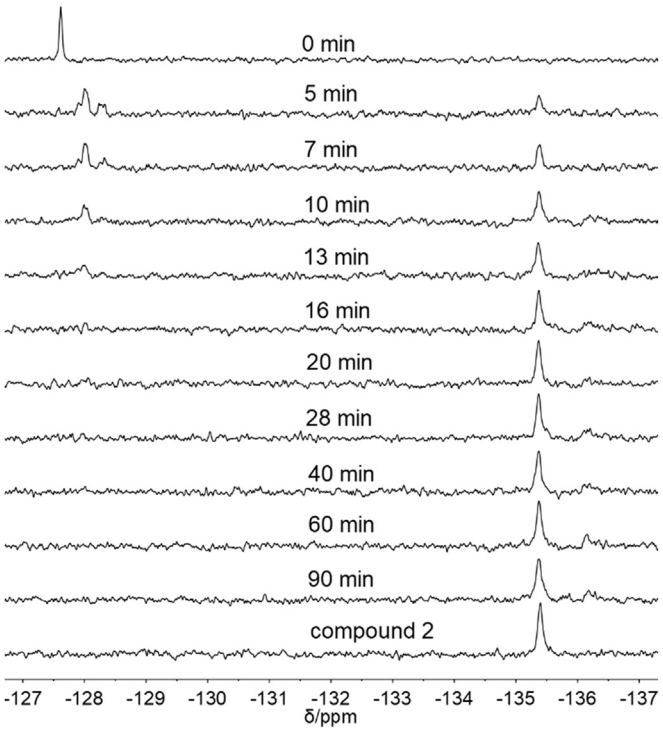

Fig. 2. ^{19}F NMR spectra (high field) change of probe 1 (200 μM) upon addition of 5 equiv. of Cys. Each spectrum was measured in HEPES buffer solution (pH 7.4, 20 mM) with 30% acetonitrile and 5% D_2O at 25 °C by 24 scans.

shift of probe 1 at $\delta = -127.6$ ppm disappeared quickly. However, new chemical shifts at -128.5 ppm, -128.3 ppm for Hcy and -128.4 ppm, -128.1 ppm for GSH were observed (Fig. S9). Importantly, the signal at $\delta = -135.4$ ppm was not observed even after 90 min by ^{19}F NMR under the test conditions, which is the significant difference with that of Cys. Additionally, higher concentrations of Hcy and GSH were investigated by time-dependent ^{19}F NMR spectra. For example, similar results were obtained when 10 and 20 equiv. of Hcy (Fig. S10) and GSH (Fig. S11) were added.

All the above results from ^{19}F NMR clearly displayed that probe 1 responds fast to Cys, Hcy and GSH and produces different ^{19}F NMR chemical shift signals (Table S1), suggesting biothiols initially involved in the reaction of conjugate addition of sulfhydryl group to an α, β-unsaturated carbonyl moiety of probe 1. However, only Cys significantly induced the appearance of signal $\delta = -135.4$ ppm, which indicate the subsequent intramolecular cyclization reaction. Thus, we anticipated that the response of probe 1 toward biothiols involved in the chemical structure transformation caused by the reaction of initially conjugate addition and subsequently intramolecular cyclization [22-26]. The difference found in the cleavage of acryloyl group, which may be reasoned by Hcy and GSH is efficient in the initial nucleophilic attack but inefficient in the subsequent ester bond cleavage reaction due to the different pK_a value of Cys (pK_a: 8.30), Hcy (pK_a: 8.87) and GSH (pK_a: 9.20) [64]

3.4. Proposed reaction mechanism

To shed light on the mechanism, we performed HPLC-UV analysis coupled with High Resolution Mass Spectrometry (HRMS) experiments. Under the test conditions, the HPLC spectrum of probe 1 displays a signal at the retention time of 14.2 min by monitoring the λ_{max} at 398 nm. Upon addition of 10 equivalents Cys, two new signals at retention time of 1.8 min and 6.7 min were found in the HPLC spectrum (Fig. S12). As time goes by, the signals at retention times of 14.2 min and 1.8 min completely disappeared. Concomitantly, the signal intensity at a retention time 6.7 min increased, which was confirmed as the predicted compound 2 by comparison with the authenticated sample. The above result indicates that the signals at retention times of 1.8 min and 6.7 min could be attributed to the intermediate and product 2, respectively. Furthermore, HRMS analysis of these three signals shows the corresponding peaks at $m/z = 497.1288$, 322.0986 and 376.1095, which are consistent with the molecular weight of the expected [1-Cys + H^+] intermediate (calcd 497.1289), compound [2 + H^+] (calcd 322.0986) and probe [1 + H^+] (calcd 376.1092) (Fig. S13). In the experiments of probe 1 with Hcy and GSH, the same HPLC peak at 6.7 min and its corresponding HRMS result were also observed (Fig. S14). The results reveled compound 2 was produced by the reaction of probe 1 with Hcy and GSH. However, this signal was not observed when using ^{19}F NMR to monitor the reaction process of probe 1 with Hcy and GSH under test conditions. The reason could be the different sensitivity of ^{19}F NMR, HPLC and HRMS. Additionally, the HPLC peaks at 2.2 min for Hcy and 1.7 min for GSH could be attributed to the intermediates [1-Hcy] and [1-GSH], respectively, which also were verified by HRMS analysis (Fig. S15). These results show that the reactions of probe 1 with Cys, Hcy and GSH were thiol-addition reactions with subsequent intramolecular cyclization, but the reactions of probe 1 with Hcy and GSH is much slower than that of Cys. Based on these studies, we hypothesized the reaction mechanism of probe 1 with Cys was illustrated in Scheme 3.

3.5. Selectivity and sensitivity studies of probe 1

The selectivity of probe 1 towards Cys, Hcy and GSH has also been investigated with various other species (Fig. 3). As shown in Fig. 3, it

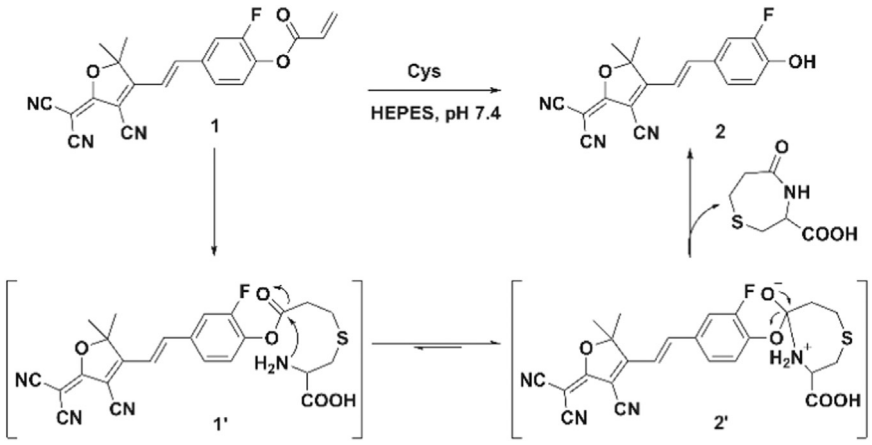

Scheme 3. Proposed reaction mechanism of probe 1 and Cys.

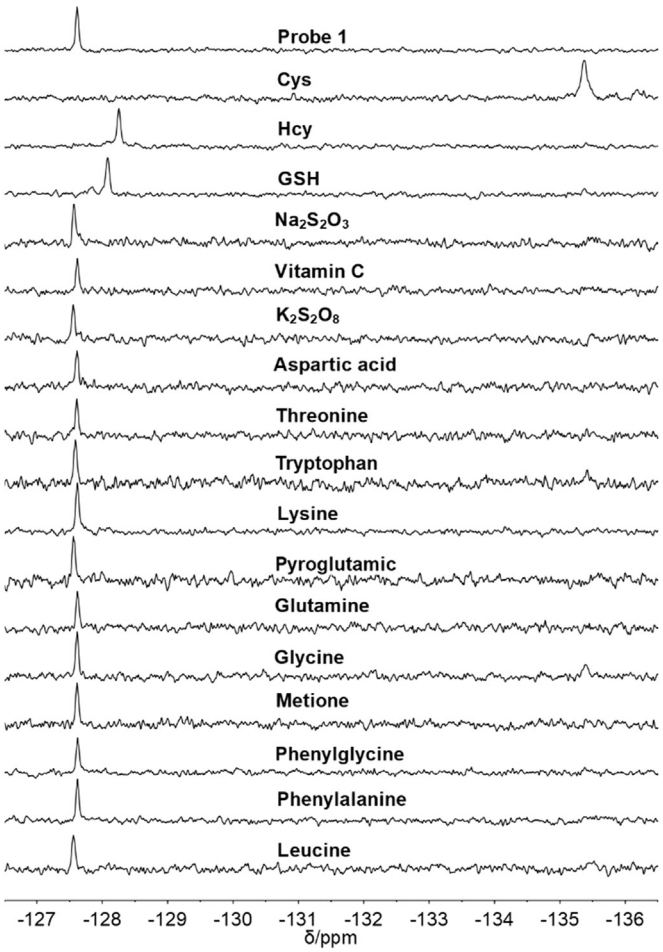

Fig. 3. ^{19}F NMR spectra of probe 1 (200 μM) in the presence of various analytes (the concentration of Cys, Hcy and GSH were 1000 μM, the rest analytes were 2000 μM). Each spectrum was obtained by 24 scans in HEPES buffer solution (pH 7.4, 20 mM) with 30% acetonitrile and 5% D_2O at 25 °C.

was found that only the Cys, Hcy and GSH induced the significant ^{19}F chemical shift change of probe 1, whereas the other species such as $Na_2S_2O_3$, vitamin C, $K_2S_2O_8$, Asp, Thr, Trp, Lys, pyroglutamic, Glu, Gly, Met, phenylglycine, phenylalanine and Leu caused no significant effect of chemical shift change. The results showed probe 1 is highly selective for biothiols over other test species.

To evaluate the sensitivity of probe 1 towards biothiols (Fig. S16), the reaction of probe 1 with Cys at low concentration was performed. Under the test conditions, the peak at − 135.4 ppm was clearly shown up after 4800 signal averages. The result revealed the probe 1 can react with Cys at low concentrations, and also can be detected by ^{19}F NMR.

3.6. Simultaneous detection

To demonstrate the ability of probe 1 to achieve simultaneous resolution of Cys, Hcy and GSH in a mixture, extraordinary experiment was further carried out. The Cys, Hcy and GSH mixed solution was added to the solution of probe 1 in 20 mM HEPES buffer solution with 30% acetonitrile and 5% D_2O, and recorded by the ^{19}F NMR with time course. As shown in the Fig. 4, the signal at − 127.6 ppm disappeared quickly upon addition to the mixture. Concomitantly, the signals at − 128.1 ppm (and − 128.4 ppm), − 128.3 ppm (and − 128.5 ppm)

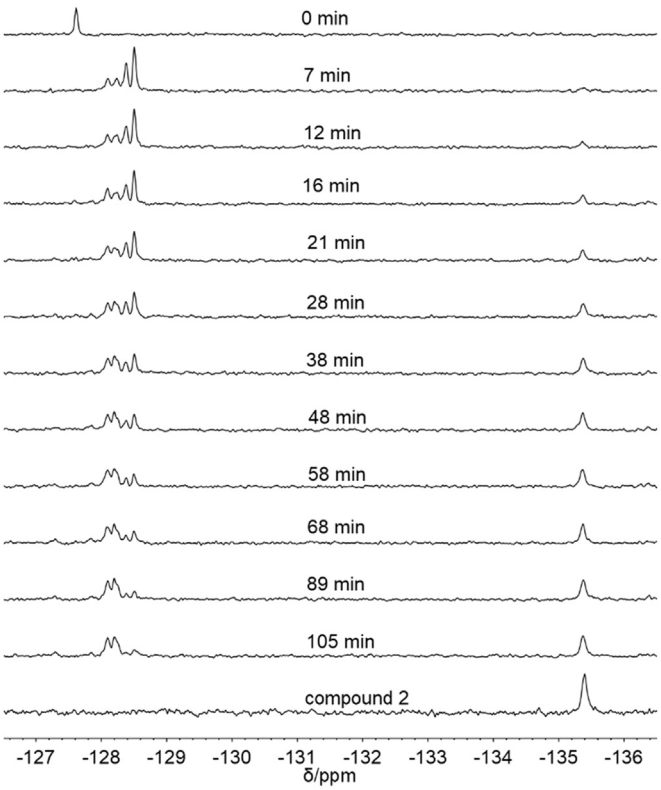

Fig. 4. ^{19}F NMR chemical shift change of probe 1 (600 μM) upon addition of the mixture of Cys (200 μM), Hcy (400 μM) and GSH (400 μM). Each spectrum was obtained by 24 scans in HEPES buffer solution (pH 7.4, 20 mM) with 30% acetonitrile and 5% D_2O at 25 °C.

and − 135.4 ppm were all observed, which were assigned to the signals of probe 1 with Hcy, GSH and Cys, respectively. As time increased, a similar process occurred with the signals at − 128.4 ppm and − 128.5 ppm decreasing gradually with concomitant ingrowth of the signals at δ = − 128.1 ppm, − 128.3 ppm and − 135.4 ppm.

Finally, we sought to explore the application of probe 1 for Cys, Hcy and GSH detection in bovine serum containing solution. It is clear that probe 1 is stable in the bovine serum containing solution during the test (Fig. S17). After addition of individual or mixture of Cys, Hcy and GSH solution, the ^{19}F NMR spectra (Fig. S18 and S19) show the quite similar changes as that observed in the above experiments. For example, upon addition of the mixture of Cys, Hcy and GSH solution, the signal of probe 1 at − 127.6 ppm disappeared quickly, while five new signals at − 128.1 ppm, − 128.3 ppm, − 128.4 ppm, − 128.5 ppm and − 135.4 ppm were observed. Among them, the intensity of signals at − 128.4 ppm, − 128.5 ppm gradually declined and the rest increased until reach the plateau. These results demonstrate that probe 1 has extraordinary ability to simultaneously discriminate Cys, Hcy, and GSH in mixed solutions, even in the presence of bovine serum. One appealing feature of this probe is its reaction resolving ability provided by the reactive functional group of sulfhydryl, which increases its success in resolving these challenging analytes. In contrast to other conventional methods, this method is not only capable of discriminating Cys, Hcy, and GSH, but also can resolve them in mixed solutions.

4. Conclusions

In summary, we have developed a new chemosensory platform based on ^{19}F NMR spectroscopy by using thiols-specific reaction. The reaction of probe 1 with biothiols produces distinct and precise ^{19}F NMR chemical shifts. This approach provides simple and robust differentiation of biothiols that are not easily resolved by other methods. The key to the success of this approach is the specific reaction of probe with biothiols, and detected and differentiated by fluorine probes. We expect the combination of the current strategy and diversified supramolecular scaffolds will produce a powerful sensing platform that addresses these structure similar biomolecules relevant to biological chemistry.

Acknowledgment

This work is supported by National Natural Science Foundation of China (81625011, 81227902), National Key R&D Program of China (2016YFC1304700 , 2017YFA0505400), Key Research Program of Frontier Sciences, CAS (QYZDY-SSW-SLH018) and National Program for Support of Eminent Professionals (National Program for Support of Top-notch Young Professionals).

Appendix A. Supporting information

Supplementary data associated with this article can be found in the online version at http://dx.doi.org/10.1016/j.talanta.2018.03.039.

References

[1] X. Chen, Y. Zhou, X.J. Peng, J. Yoon, Fluorescent and colorimetric probes for detection of thiols, Chem. Soc. Rev. 39 (2010) 2120–2135.
[2] S. Shahrokhian, Lead phthalocyanine as a selective carrier for preparation of a cysteine-selective electrode, Anal. Chem. 73 (2001) 5972–5978.
[3] T.P. Dalton, H.G. Shertzer, A. Puga, Regulation of gene expression by reactive oxygen, Annu. Rev. Pharmacol. Toxicol. 39 (1999) 67–101.
[4] B.M. Lomaestro, M. Malone, Glutathione in health and disease: pharmacotherapeutic issues, Ann. Pharmacother. 29 (1995) 1263–1273.
[5] J. Vacek, B. Klejdus, J. Petrlova, L. Lojkova, V. Kuban, A hydrophilic interaction chromatography coupled to a mass spectrometry for the determination of glutathione in plant somatic embryos, Analyst 131 (2006) 1167–1174.
[6] W. Chen, Y. Zhao, T. Seefeldt, X. Guan, Determination of thiols and disulfides via HPLC quantification of 5-thio-2-nitrobenzoic acid, J. Pharm. Biomed. Anal. 48 (2008) 1375–1380.
[7] Y.-Y. Ling, X.-F. Yin, Z.-L. Fang, Simultaneous determination of glutathione and reactive oxygen species in individual cells by microchip electrophoresis, Electrophoresis 26 (2005) 4759–4766.
[8] T. Inoue, J.R. Kirchhoff, Determination of thiols by capillary electrophoresis with amperometric detection at a coenzyme pyrroloquinoline quinone modified electrode, Anal. Chem. 74 (2002) 1349–1354.
[9] P. Calvo-Marzal, K.Y. Chumbimuni-Torres, N.F. Höehr, L.T. Kubota, Determination of glutathione in hemolysed erythrocyte with amperometric sensor based on TTF-TCNQ, Clin. Chim. Acta 371 (2006) 152–158.
[10] A. Nezamzadeh-Ejhieh, H.-S. Hashemi, Voltammetric determination of cysteine using carbon paste electrode modified with Co(II)-Y zeolite, Talanta 88 (2012) 201–208.
[11] A. Waseem, M. Yaqoob, A. Nabi, Flow-injection determination of cysteine in pharmaceuticals based on luminol-persulphate chemiluminescence detection, Luminescence 23 (2008) 144–149.
[12] T. Pérez-Ruiz, C. Martínez-Lozano, V. Tomás, J. Carpena, Spectrofluorimetric flow injection method for the individual and successive determination of L-cysteine and L-cystine in pharmaceutical and urine samples, Analyst 117 (1992) 1025–1028.
[13] N. Burford, M.D. Eelman, D.E. Mahony, M. Morash, Definitive identification of cysteine and glutathione complexes of bismuth by mass spectrometry: assessing the biochemical fate of bismuth pharmaceutical agents, Chem. Commun. 7 (2003) 146–147.
[14] C. Atsriku, C.C. Benz, G.K. Scott, B.W. Gibson, M.A. Baldwin, Quantification of cysteine oxidation in human estrogen receptor by mass spectrometry, Anal. Chem. 79 (2007) 3083–3090.
[15] K. Xu, Y. Zhang, B. Tang, J. Laskin, P.J. Roach, H. Chen, Study of highly selective and efficient thiol derivatization using selenium reagents by mass spectrometry, Anal. Chem. 82 (2010) 6926–6932.
[16] S. Yang, W. Jiang, L. Ren, Y. Yuan, B. Zhang, Q. Luo, Q. Guo, L.-S. Bouchard, M. Liu, X. Zhou, Biothiol xenon MRI sensor based on thiol-addition reaction, Anal. Chem. 88 (2016) 5835–5840.
[17] Q. Zeng, Q. Guo, Y. Yuan, Y. Yang, B. Zhang, L. Ren, X. Zhang, Q. Luo, M. Liu, L.-S. Bouchard, X. Zhou, Mitochondria targeted and intracellular biothiol triggered hyperpolarized ^{129}Xe magnetofluorescent biosensor, Anal. Chem. 89 (2017) 2288–2295.
[18] C. Yin, F. Huo, J. Zhang, R. Martínez-Máñez, Y. Yang, H. Lv, S. Li, Thiol-addition reactions and their applications in thiol recognition, Chem. Soc. Rev. 42 (2013) 6032–6059.
[19] J. Wang, H.-B. Liu, Z. Tong, C.-S. Ha, Fluorescent/luminescent detection of natural amino acids by organometallic systems, Coord. Chem. Rev. 303 (2015) 139–184.
[20] M.E. Jun, B. Roy, K.H. Ahn, "Turn-on" fluorescent sensing with "reactive" probes, Chem. Commun. 47 (2011) 7583–7601.
[21] B.K. McMahon, T. Gunnlaugsson, Selective detection of the reduced form of glutathione (GSH) over the oxidized (GSSG) form using a combination of glutathione reductase and a Tb(III)-cyclen maleimide based lanthanide luminescent 'Switch On' assay, J. Am. Chem. Soc. 134 (2012) 10725–10728.
[22] C. Han, H. Yang, M. Chen, Q. Su, W. Feng, F. Li, Mitochondria-targeted near-infrared fluorescent off–on probe for selective detection of cysteine in living cells and in vivo, ACS Appl. Mater. Interfaces 50 (2015) 27968–27975.
[23] W. Niu, L. Guo, Y. Li, S. Shuang, C. Dong, M.S. Wong, Highly selective two-photon fluorescent probe for ratiometric sensing and imaging cysteine in mitochondria, Anal. Chem. 88 (2016) 1908–1914.
[24] J. Zhang, J. Wang, J. Liu, L. Ning, X. Zhu, B. Yu, X. Liu, X. Yao, H. Zhang, Near-infrared and naked-eye fluorescence probe for direct and highly selective detection of cysteine and its application in living cells, Anal. Chem. 87 (2015) 4856–4863.
[25] X.F. Yang, Y. Guo, R.M. Strongin, Conjugate addition/cyclization sequence enables selective and simultaneous fluorescence detection of cysteine and homocysteine, Angew. Chem. Int. Ed. 50 (2011) 10690–10693.
[26] Z. Guo, S.W. Nam, S. Park, J.Y. Yoon, A highly selective ratiometric near-infrared fluorescent cyanine sensor for cysteine with remarkable shift and its application in bioimaging, Chem. Sci. 3 (2012) 2760–2765.
[27] Q. Miao, Q. Li, Q. Yuan, L. Li, Z. Hai, S. Liu, G. Liang, Discriminative fluorescence sensing of biothiols in vitro and in living cells, Anal. Chem. 87 (2015) 3460–3466.
[28] H. Lv, X. Yang, Y. Zhong, Y. Guo, Z. Li, H. Li, Native chemical ligation combined with spirocyclization of benzopyrylium dyes for the ratiometric and selective fluorescence detection of cysteine and homocysteine, Anal. Chem. 86 (2014) 1800–1807.
[29] S.-Y. Lim, K.-H. Hong, D.I. Kim, H. Kwon, H.-J. Kim, Tunable heptamethine-Azo dye conjugate as an NIR fluorescent probe for the selective detection of mitochondrial glutathione over cysteine and homocysteine, J. Am. Chem. Soc. 136 (2014) 7018–7025.
[30] T. Bao, Q. Li, B. Liu, F. Du, J. Tian, H. Wang, Y. Wang, R. Bai, Conjugated polymers containing a 2,2′-biimidazole moiety–a novel fluorescent sensing platform, Chem. Commun. 48 (2012) 118–120.
[31] L.-Y. Niu, Y.-S. Guan, Y.-Z. Chen, L.-Z. Wu, C.-H. Tung, Q.-Z. Yang, BODIPY-based ratiometric fluorescent sensor for highly selective detection of glutathione over cysteine and homocysteine, J. Am. Chem. Soc. 134 (2012) 18928–18931.
[32] J. Liu, Y.-Q. Sun, Y. Huo, H. Zhang, L. Wang, P. Zhang, D. Song, Y. Shi, W. Guo, Simultaneous fluorescence sensing of Cys and GSH from different emission channels, J. Am. Chem. Soc. 136 (2014) 574–577.
[33] X.-F. Yang, Q. Huang, Y. Zhong, Z. Li, H. Li, M. Lowry, J.O. Escobedo, R.M. Strongin, A dual emission fluorescent probe enables simultaneous detection of glutathione and cysteine/homocysteine, Chem. Sci. 5 (2014) 2177–2183.
[34] S. Gündüz, T. Savić, R. Pohmann, N.K. Logothetis, K. Scheffler, G. Angelovski, Ratiometric method for rapid monitoring of biological processes using bioresponsive MRI contrast agents, ACS Sens. 1 (2016) 483–487.

[35] M.G. Shapiro, G.G. Westmeyer, P.A. Romero, J.O. Szablowski, B. Küster, A. Shah, C.R. Otey, R. Langer, F.H. Arnold, A. Jasanoff, Directed evolution of a magnetic resonance imaging contrast agent for noninvasive imaging of dopamine, Nat. Biotechnol. 28 (2010) 264–270.
[36] A. Bar-Shir, L. Avram, S. Yariv-Shoushan, D. Anaby, S. Cohen, N. Segev-Amzaleg, D. Frenkel, O. Sadan, D. Offen, Y. Cohen, Alginate-coated magnetic nanoparticles for noninvasive MRI of extracellular calcium, NMR Biomed. 27 (2014) 774–783.
[37] C.S. Bonnet, F. Caillé, A. Pallier, J.-F. Morfin, S. Petoud, F. Suzenet, É. Tóth, Mechanistic studies of Gd^{3+}-based MRI contrast agents for Zn^{2+} detection: towards rational design, Chem. Eur. J. 20 (2014) 10959–10969.
[38] A. Hai, L.X. Cai, T. Lee, V.S. Lelyveld, A. Jasanoff, Molecular fMRI of serotonin transport, Neuron 92 (2016) 754–765.
[39] L.M. De Leon-Rodriguez, A.J.M. Lubag, C.R. Malloy, G.V. Martinez, R.J. Gillies, A.D. Sherry, Responsive MRI agents for sensing metabolism in vivo, Acc. Chem. Res. 42 (2009) 948–957.
[40] S. Viswanathan, Z. Kovacs, K.N. Green, S.J. Ratnakar, A.D. Sherry, Alternatives to gadolinium-based metal chelates for magnetic resonance imaging, Chem. Rev. 110 (2010) 2960–3018.
[41] A. Razgulin, N. Ma, J. Rao, Strategies for in vivo imaging of enzyme activity: an overview and recent advances, Chem. Soc. Rev. 40 (2011) 4186–4216.
[42] P. Verwilst, S. Park, B. Yoon, J.S. Kim, Recent advances in Gd-chelate based bimodal optical/MRI contrast agents, Chem. Soc. Rev. 44 (2015) 1791–1806.
[43] A.D. Sherry, Y.K. Wu, Following the Ca^{2+} roadmap to photocaged complexes for Zn^{2+} and beyond, Curr. Opin. Chem. Biol. 17 (2013) 167–174.
[44] I. Tirotta, V. Dichiarante, C. Pigliacelli, G. Cavallo, G. Terraneo, F.B. Bombelli, P. Metrangolo, G. Resnati, ^{19}F Magnetic resonance imaging (MRI): from design of materials to clinical applications, Chem. Rev. 115 (2015) 1106–1129.
[45] J.-X. Yu, R.R. Hallac, S. Chiguru, R.P. Mason, New frontiers and developing applications in ^{19}F NMR, Prog. Nucl. Magn. Reson. Spectrosc. 70 (2013) 25–49.
[46] R.P. Mason, Transmembrane pH gradients in vivo: measurements using fluorinated vitamin B6 derivatives, Curr. Med. Chem. 6 (1999) 481–499.
[47] A.M. Kenwright, I. Kuprov, E. De Luca, D. Parker, S.U. Pandya, P.K. Senanayake, D.G. Smith, ^{19}F NMR based pH probes: lanthanide(III) complexes with pH-sensitive chemical shifts, Chem. Commun. (2008) 2514–2516.
[48] G.A. Smith, R.T. Hesketh, J.C. Metcalfe, J. Feeney, P.G. Morris, Intracellular calcium measurements by ^{19}F NMR of fluorine-labeled chelators, Proc. Natl. Acad. Sci. USA 80 (1983) 7178–7182.
[49] P. Harvey, K.H. Chalmers, E. De Luca, A. Mishra, D. Parker, Paramagnetic ^{19}F chemical shift probes that respond selectively to calcium or citrate levels and signal ester hydrolysis, Chem. Eur. J 18 (2012) 8748–8757.
[50] T. Doura, A. Qi, F. Sugihara, T. Matsuda, S. Sando, p-Aminophenyl alkyl ether-based ^{19}F MRI probe for specific detection and imaging of hypochlorite ion, Chem. Lett. 12 (2011) 1357–1359.
[51] T. Doura, R. Hata, H. Nonaka, F. Sugihara, Y. Yoshioka, S. Sando, An adhesive ^{19}F MRI chemical probe allows signal off-to-on-type molecular sensing in a biological environment, Chem. Commun. 49 (2013) 11421–11423.
[52] A.A. Bobko, S.V. Sergeeva, E.G. Bagryanskaya, A.L. Markel, V.V. Khramtsov, V.A. Reznikov, N.G. Kolosova, ^{19}F NMR measurements of NO production in hypertensive ISIAH and OXYS rats, Biochem. Biophys. Res. Commun. 330 (2005) 367–370.
[53] R.P. Mason, R.L. Nunnally, P.P. Antich, Tissue oxygenation: a novel determination using ^{19}F surface coil NMR spectroscopy of sequestered perfluorocarbon emulsion, Magn. Reson. Med. 18 (1991) 71–79.
[54] K.A. Krohn, J.M. Link, R.P. Mason, Molecular imaging of hypoxia, J. Nucl. Med. 49 (2008) 129S–148S.
[55] K. Yamaguchi, R. Ueki, H. Nonaka, F. Sugihara, T. Matsuda, S. Sando, Design of chemical shift-switching ^{19}F magnetic resonance imaging probe for specific detection of human monoamine oxidase A, J. Am. Chem. Soc. 133 (2011) 14208–14211.
[56] K. Matsuo, R. Kamada, K. Mizusawa, H. Imai, Y. Takayama, M. Narazaki, T. Matsuda, Y. Takaoka, I. Hamachi, Specific detection and imaging of enzyme activity by signal-amplifiable self-assembling ^{19}F MRI probes, Chem. Eur. J. 19 (2013) 12875–12883.
[57] Y. Takaoka, T. Sakamoto, S. Tsukiji, M. Narazaki, T. Matsuda, H. Tochio, M. Shirakawa, I. Hamachi, Self-assembling nanoprobes that display off/on ^{19}F nuclear magnetic resonance signals for protein detection and imaging, Nat. Chem. 1 (2009) 557–561.
[58] J. Axthelm, H. Görls, U.S. Schubert, A. Schiller, Fluorinated boronic acid-appended bipyridinium salts for diol recognition and discrimination via ^{19}F NMR barcodes, J. Am. Chem. Soc. 137 (2015) 15402–15405.
[59] Y. Zhao, T.M. Swager, Detection and differentiation of neutral organic compounds by ^{19}F NMR with a tungsten calix[4]arene imido complex, J. Am. Chem. Soc. 135 (2013) 18770–18773.
[60] Y. Zhao, T.M. Swager, Simultaneous chirality sensing of multiple amines by ^{19}F NMR, J. Am. Chem. Soc. 37 (2015) 3221–3224.
[61] Y. Zhao, L. Chen, T.M. Swager, Simultaneous identification of neutral and anionic species in complex mixtures without separation, Angew. Chem. Int. Ed. 55 (2016) 917–921.
[62] M. Ipuy, C. Billon, G. Micouin, J. Samarut, C. Andraud, Y. Bretonnière, Fluorescent push–pull pH-responsive probes for ratiometric detection of intracellular pH, Org. Biomol. Chem. 12 (2014) 3641–3648.
[63] J.-T. Hou, J. Yang, K. Li, K. Yu, X.-Q. Yu, A colorimetric and red emissive fluorescent probe for cysteine and its application in bioimaging, Sens. Actuators B 214 (2015) 92–100.
[64] M. Iciek, G. Chwatko, E. Lorenc-Koci, E. Bald, L. Wlodek, Plasma levels of total, free and protein bound thiols as well as sulfane sulfur in different age groups of rats, Acta Biochim. Pol. 51 (2004) 815–824.